RESEARCH ARTICLE

Cannabigerolic Acid (CBGA) Inhibits the TRPM7 Ion Channel Through its Kinase Domain

Sayuri Suzuki [1],*, Clay Wakano [1], Mahealani K. Monteilh-Zoller[1],
Aaron J. Cullen[1], Andrea Fleig[1,2,3], Reinhold Penner[1,2,3],*

[1]Center for Biomedical Research, The Queen's Medical Center, 1301 Punchbowl St., Honolulu, HI 96813, USA,
[2]University of Hawaii Cancer Center, 651 Ilalo St., Honolulu, HI 96813, USA and [3]John A. Burns School of
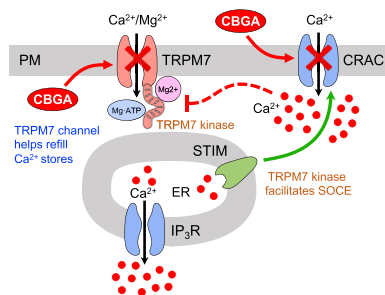Medicine, University of Hawaii, 651 Ilalo St., Honolulu, HI 96813, USA

*Address correspondence to R.P. (e-mail: rpenner@hawaii.edu), S.S. (e-mail: sayuris@hawaii.edu)

Abstract

Cannabinoids are a major class of compounds produced by the plant Cannabis sativa. Previous work has demonstrated that
the main cannabinoids cannabidiol (CBD) and tetrahydrocannabinol (THC) can have some beneficial effects on pain,
inflammation, epilepsy, and chemotherapy-induced nausea and vomiting. While CBD and THC represent the two major
plant cannabinoids, some hemp varieties with enzymatic deficiencies produce mainly cannabigerolic acid (CBGA). We
recently reported that CBGA has a potent inhibitory effect on both Store-Operated Calcium Entry (SOCE) via inhibition of
Calcium Release-Activated Calcium (CRAC) channels as well as currents carried by the channel-kinase TRPM7. Importantly,
CBGA prevented kidney damage and suppressed mRNA expression of inflammatory cytokines through inhibition of these
mechanisms in an acute nephropathic mouse model. In the present study, we investigate the most common major and
minor cannabinoids to determine their potential efficacy on TRPM7 channel function. We find that approximately half of
the tested cannabinoids suppress TRPM7 currents to some degree, with CBGA having the strongest inhibitory effect on
TRPM7. We determined that the CBGA-mediated inhibition of TRPM7 requires a functional kinase domain, is sensitized by
both intracellular Mg·ATP and free Mg^{2+} and reduced by increases in intracellular Ca^{2+}. Finally, we demonstrate that CBGA
inhibits native TRPM7 channels in a B lymphocyte cell line. In conclusion, we demonstrate that CBGA is the most potent
cannabinoid in suppressing TRPM7 activity and possesses therapeutic potential for diseases in which TRPM7 is known to
play an important role such as cancer, stroke, and kidney disease.

Key words: cannabinoids; cannabigerolic acid (CBGA); Transient Receptor Potential Melastatin 7 (TRPM7)

Introduction

Cannabis sativa has a rich history as a plant-based medicine, used to treat conditions like chronic pain, nausea, anxiety, insomnia, anorexia, and muscle spasms.[1,2] It is also used in the treatment of chronic disorders such as autoimmune and neurodegenerative diseases,[3] cancer,[4,5] multiple sclerosis,[6–8] and epilepsy.[9–11] This broad therapeutic efficacy underscores the importance of elucidating the underlying mechanisms behind the diverse benefits of cannabis. Compositionally, the cannabis plant is dominated by a large class of natural products known as phytocannabinoids, which possess anti-inflammatory and analgesic properties.[12,13] Like the plant itself, the phytocannabinoids act through a multitude of mechanisms. These include G-protein-coupled receptors such as cannabinoid receptors type 1 (CB1) and type 2 (CB2) or CB1/CB2-independent pathways.[14] In addition, cannabinoids have been found to affect other biological targets, including members of the transient receptor potential (TRP) family of ion channels.[15,16]

Cannabigerolic acid (CBGA) is the acidic form cannabigerol (CBG) and represents the biosynthetic precursor to a vast number of cannabinoids, including tetrahydrocannabinol (THC) and cannabidiol (CBD). Like CBD, cannabigerolic acid (CBGA) has been found to have anticonvulsant effects in mouse models of epilepsy.[17] CBGA has been reported to be a dual PPARα/γ agonist with the potential to treat metabolic disorders such as diabetes and dyslipidemia.[18] Preclinical findings show that CBG, the decarboxylated version of CBGA, reduces intraocular pressure, possesses antioxidant, anti-inflammatory, and antitumoral activities, and has antianxiety, neuroprotective, dermatological, and appetite-stimulating effects.[19] Both CBGA and CBG have neuroprotective properties in Parkinson's disease model[20,21]; however, the mechanisms of action and pharmacological effects remain to be elucidated in more detail.

TRPM7 is a member of the transient receptor potential melastatin (TRPM) family of ion channels and is composed of a 6 transmembrane spanning ion channel domain and a functional serine/threonine kinase domain at the protein's intracellular C-terminus.[22] TRPM7 conducts a range of divalent cations such as Ca^{2+}, Mg^{2+}, Zn^{2+}, Ni^{2+}, Mn^{2+}, and Co^{2+} into cells via the channel domain.[23,24] The TRPM7 protein is expressed ubiquitously in mammals, where it is critical for regulating both organismal and cellular Mg^{2+} homeostasis. While TRPM7 knock-out is embryonic lethal,[25] dysregulated TRPM7 activity represents an important factor in a variety of diseases, including neuronal death in ischemia,[26] cardiac atrial fibrillation,[27] and renal diseases.[28–30] TRPM7 also plays a key role in several fibrotic disorders, including cardiac,[31] hepatic,[32] pulmonary,[33] and renal

fibrosis.[34] TRPM7 also drives cell proliferation, cell growth, apoptosis, and differentiation, thereby contributing to hyperproliferative diseases such as cancer.[22,35,36]

TRPM7 is suppressed by physiological amounts of intracellular adenosine triphosphate (Mg·ATP) and Mg^{2+}.[37–39] Inhibition of TRPM7's enzymatic activity by genetic modification of its endogenous kinase domain reduces the sensitivity of TRPM7 to its intracellular inhibitors Mg^{2+} and Mg·ATP.[40] The binding of Mg·ATP to the kinase domain is required to phosphorylate other protein targets, whereas TRPM7 channel domain function is not required for enzymatic activity of the TRPM7 kinase function.

Previous work has demonstrated the ability of cannabinoids to modulate calcium signaling through various TRP channels[15] and calcium release-activated calcium (CRAC) channels.[41] We recently reported that CBGA was the most potent cannabinoid suppressing store-operated calcium entry (SOCE) and IL-2 production in T cells.[41] Building upon this initial discovery, we showed that CBGA also decreased IL-2 production and ameliorated kidney inflammation in an acute nephropathic mouse model.[28] Additionally, CBGA reduced kidney fibrosis in a progressive renal fibrotic model.[28] Encouraged by this in vivo result, we explored the mechanism behind the renal-protective properties of CBGA. We showed a novel mechanism by which CBGA reduces kidney disease at least in part owing to its inhibitory action on TRPM7, indicating the potential therapeutic impact of CBGA on both acute and chronic kidney disease. In this communication we characterize the mechanistic interaction between TRPM7 and CBGA and report that the inhibitory action of CBGA on TRPM7 requires its kinase domain to remain functional and is modulated by both intracellular and Mg·ATP, free Mg^{2+}, and free Ca^{2+}.

Materials and Methods

Cell Culture

Tetracycline (Tet)-inducible HEK293-TREx cells, stably transfected with human TRPM7 (hTRPM7), were cultured in Dulbecco's Modified Eagle Medium (DMEM) (Gibco) containing 10% fetal bovine serum (FBS, Gibco), zeocin (0.4 mg/mL, Invitrogen), and blasticidin (5 μg/mL, Invitrogen). HEK293 cells stably transfected with the phosphotransferase activity-deficient point mutation in the hTRPM7 kinase domain, hTRPM7/K1648R and hTRPM7/G1799D, were cultured in the same medium. Tet-inducible human TRPM6 + human TRPM7 HEK293-TREx cells were maintained in DMEM medium containing 10% FBS, zeocin (0.4 mg/mL), blasticidin (5 μg/mL), and hygromycin (0.4 mg/mL, Chemi Cruz). Overexpression was induced by adding 1 μg/mL

tetracycline (Gibco) to the culture medium. Patch-clamp experiments were performed 18-21 h post-tetracycline induction. HEK293-TREx cells were transiently transfected with green fluorescent protein (GFP)-tagged human TRPM6 plasmid using Lipofectamine 2000 (Invitrogen). Whole-cell patch-clamp experiments were carried out 26 h post-transfection. Expression of human TRPM6 constructs was identified by green fluorescence. U266 cells were cultured in RPMI-1640 medium (Gibco) containing 10% FBS. Cells were maintained at 37°C under 5% CO_2 conditions.

Whole-cell Patch-Clamp Recording

Patch-clamp experiments were performed in the whole-cell configuration. Currents were elicited by a ramp protocol from -100 to $+100$ mV over 50 ms acquired at 0.5 kHz and a holding potential of 0 mV. Outward current amplitudes over the course of the experiment were extracted at $+80$ mV, inward currents were extracted at -80 mV, and plotted versus time. Data were normalized to cell size measured immediately after whole-cell break-in (pA/pF). Capacitance was measured using the automated capacitance cancellation function of the EPC-9 (HEKA, Germany). All values are given as mean $\pm$ SEM. Patch pipettes (Sutter Instrument, CA) were pulled and polished, had a tip resistance of 2-3 MΩ when filled with internal solution. Standard extracellular solution contained (in mM): 140 NaCl, 2.8 KCl, 2 $MgCl_2$, 1 $CaCl_2$, 10 HEPES-NaOH, and 11 Glucose (pH 7.2, 300 mOsm). Standard pipette-filling solution for screening of cannabinoids on inducible hTRPM7/HEK293 cells contained (in mM): 130 K-glutamate, 8 NaCl, 1 $MgCl_2$, 10 EGTA, and 10 HEPES-KOH. For other patch-clamp experiments using hTRPM7/HEK293 cells, internal cellular solution contained (in mM): 140 Cs-glutamate, 8 NaCl, 10 Cs-BAPTA, 10 HEPES-CsOH. Na-ATP, $MgCl_2$, and $CaCl_2$ were supplemented with desired concentrations of $[Mg \cdot ATP]_i$, $[Mg^{2+}]_i$, and $[Ca^{2+}]_I$ as calculated with Web-MaxC (https://somapp.ucdmc.ucdavis.edu/pharmacology/bers/maxchelator/webmaxc/webmaxcS.htm). For the experiments of CBGA preincubation and TRPM6/TRPM7, internal cellular solution contained (in mM): 130 Cs-glutamate, 8 NaCl, 10 Cs-BAPTA, 10 HEPES-CsOH, 1 Na-ATP, and 1.764 $MgCl_2$. Cells were incubated in extracellular solution containing 1.8 μM CBGA or acetonitrile as a control, patch-clamp was started after 10 mins and continued by 60 mins. For intracellular CBGA patch-clamp experiments, each concentration of CBGA was added in the same internal cellular solution to the experiment of CBGA preincubation. For transiently transfected TRPM6, internal solution contained (in mM): 130 Cs-glutamate, 8 NaCl, 10 Cs-BAPTA, and 10 HEPES-CsOH. For U266 cells, internal solution contained (in mM): 140 Cs-glutamate, 8 NaCl, 1 $MgCl_2$, 10 EGTA, and 10 HEPES-CsOH. All internal solutions were adjusted to pH 7.2, 300 mOsm. Cannabinoids were diluted to each concentration with the extracellular solution used for patch-clamp experiments. Acetonitrile was diluted in extracellular solution and used as a control application.

High-Throughput Screening Bioassay

U266 cells were incubated in fresh culture medium supplemented with 2 μM Fura-2-AM (Invitrogen), 0.1% Pluronic F-127 (Sigma-Aldrich), and 2 mM Probenecid (Sigma) and incubated at 37°C under 5% CO_2 for 1 h. Cells were washed 3 times with solution containing (in mM): 140 NaCl, 2.8 KCL, 10 HEPES-NaOH, 11 Glucose (pH 7.2, 300 mOsm) after Fura-2-AM incubation, fresh solution was added, 50 000 cells were plated in each well of

black 96-well plates with clear bottom (Greiner, Austria), and transferred to a kinetic plate reader (Hamamatsu FDSS-7000EX, Hamamatsu Photonics KK, Japan). Baseline fluorescence was measured for 1 min before application of cannabinoids (0, 1, 3, 5, 10, and 30 μM, respectively). After 10 min incubation with cannabinoids, 0.5 mM $MnCl_2$ was applied. Data acquisition continued for another 340 s. Fluorescence was excited at 360 nm, and emission was measured at 510 nm to visualize intracellular Mn^{2+} quench of Fura-2. Data were normalized to the point before application of $MnCl_2$ (650-659 s), and Mn^{2+} quench was measured at 661-690 s into the experiment. The 0 μM cannabinoid trace was set as maximum quench (100% TRPM7 activity) as a vehicle control.

Statistical Analysis

All values were given as means $\pm$ SEM.

Results

Cannabigerolic Acid is a Potent TRPM7 Inhibitor

Cannabinoids have previously been shown to modulate members of the TRP channels.[4,15,16,42] We previously reported that TRPM7 is involved in the progression of kidney damage and fibrosis[30] and recently found that CBGA confers a renoprotective effect at least partially through blocking of the TRPM7 ion channel.[28] We therefore performed a whole-cell patch-clamp screen of 22 pure cannabinoids at a concentration of 10 μM against the TRPM7 channel inducibly overexpressed in HEK293 cells. Figure 1 shows the strong inhibition of TRPM7 in response to various cannabinoids applied extracellularly for 120 s. Figure 1A illustrates the averaged temporal development of TRPM7 outward currents at $+80$ mV derived from high-resolution outwardly rectifying membrane currents evoked by voltage ramps spanning -100 to $+100$ mV over 50 ms (Figure 1C). The outward currents under our experimental conditions are carried by monovalent Cs^+, whereas the much smaller inward currents are carried by divalent cations Ca^{2+} and Mg^{2+}. Application of 10 μM CBGA completely blocked both the outward currents (Figure 1A) as well the much smaller inward currents as illustrated in a typical individual cell for the $+80$ and -80 mV (Figures 1A and B).

For convenience reasons and due to their larger amplitudes, we analyzed the effects of 22 cannabinoids on TRPM7 outward currents. Examples of the inhibitory effects of various cannabinoids applied at 10 μM are illustrated in Figure 1D and the bar graph in Figure 1E quantifies the efficacy of the various cannabinoids by plotting the relative amplitudes of TRPM7 outward currents at 260 s into the experiment. The acidic versions of cannabinoids (except CBDVA) inhibited TRPM7 activity by more than 75% (Figure 1E; blue bars) and most of the decarboxylated cannabinoids had no significant effect, except for CBG which had a modest inhibition of 43% (Figure 1E; red bars). However, 2 varinol forms of cannabinoids, cannabigerovarin (CBGV) and cannabidivarin (CBDV) strongly suppressed TRPM7 current activity by 81% and 93%, respectively.

Since CBGA and CBDV exhibited the strongest inhibition to TRPM7, we next performed experiments to assess their concentration-response behavior on TRPM7 (Figure 2). At a concentration of 10 μM, CBDV completely suppressed TRPM7 currents (Figure 2A; purple circles), whereas 3 μM CBDV inhibited 40% (Figure 2A; blue circles) and 1 μM resulted in 11% inhibition (Figure 2A; red circles). The dose-response curve fitted
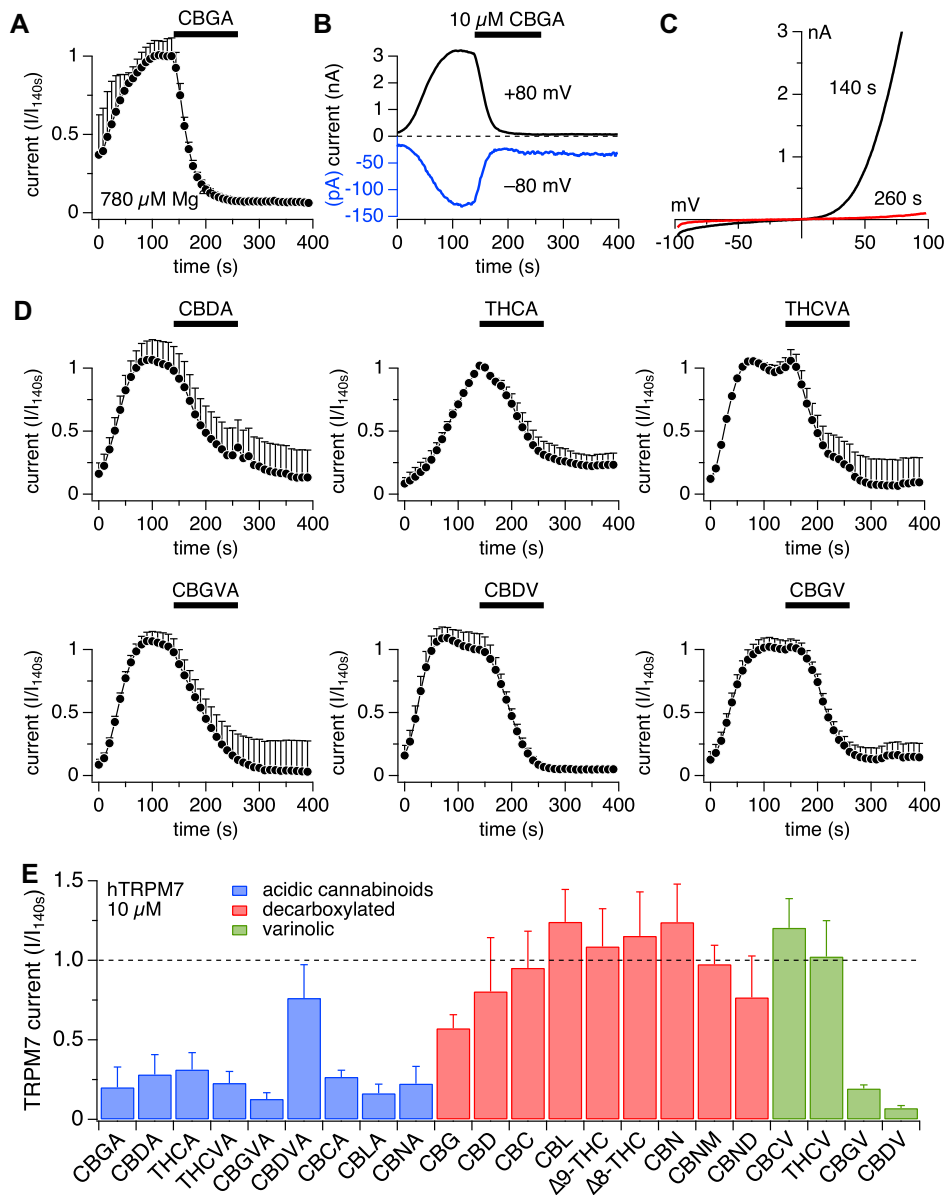
Figure 1. Cannabinoids are potent inhibitors of TRPM7 currents. The inhibitory effect of cannabinoids on TRPM7 current was assessed in whole-cell patch-clamp recordings on hTRPM7 overexpressed in HEK293 cells. In all experiments, the intracellular solution contained free Mg^{2+} at 780 μM with no added Mg·ATP. Cannabinoids were applied extracellularly at 10 μM from 140 to 260 s (black bars). Average TRPM7-mediated outward currents at +80 mV were extracted from ramp currents evoked by voltage ramps (−100 to +100 mV) delivered at 0.5 Hz and plotted as a function of time. The data points were normalized to the time point of cannabinoid application (140 s). (**A**) Inhibition of TRPM7 outward currents by cannabigerolic acid (CBGA) at +80 mV. (**B**) Outward and inward currents (at +80 and −80 mV; note the different y-axes scales) taken from a typical cell taken from (**A**), illustrating that CBGA inhibited both inward and outward currents. (**C**) High-resolution currents as a function voltage evoked by voltage ramps of −100 to +100 mV from the same cell as in (**B**) before (140 s) and after application of CBGA (260 s). (**D**) Average TRPM7 outward currents at +80 mV (*n* = 3-4) exposed to various cannabinoids (only cannabinoids with strong inhibition illustrated). (**E**) Bar graph comparing the remaining TRPM7 currents at the end of each cannabinoid application (260 s).

to these data yielded a half-maximal inhibitory concentration (IC_{50}) of CBDV of 3.4 ± 0.2 μM (Figure 2C; black). Similarly, 1 μM CBGA suppressed 35% of TRPM7 (Figure 2B; red circles), 0.3 μM inhibited TRPM7 by 26% (Figure 2B; green circles), and the calculated IC_{50} was 1.8 ± 0.6 μM (Figure 2C; red circles). Taken together, these data suggest that CBDV and CBGA provide a strong and rapid block of TRPM7 currents in a dose-dependent manner and therefore emerge as the most potent inhibitors of TRPM7.

We noticed that the inhibition of TRPM7 by low doses of CBGA was slow and accompanied by a slow and small increase in cell membrane capacitance 0.3-0.6 pF at concentrations of 5-10 μM (data not shown), indicating that the compound might partition into and possibly cross the plasma membrane to inhibit TRPM7. In the absence of a steady-state inhibition during the 120 s acute extracellular application of CBGA, the cannabinoid's true IC_{50} value could well be lower if applied for longer times and/or administered intracellularly. To test this notion, we
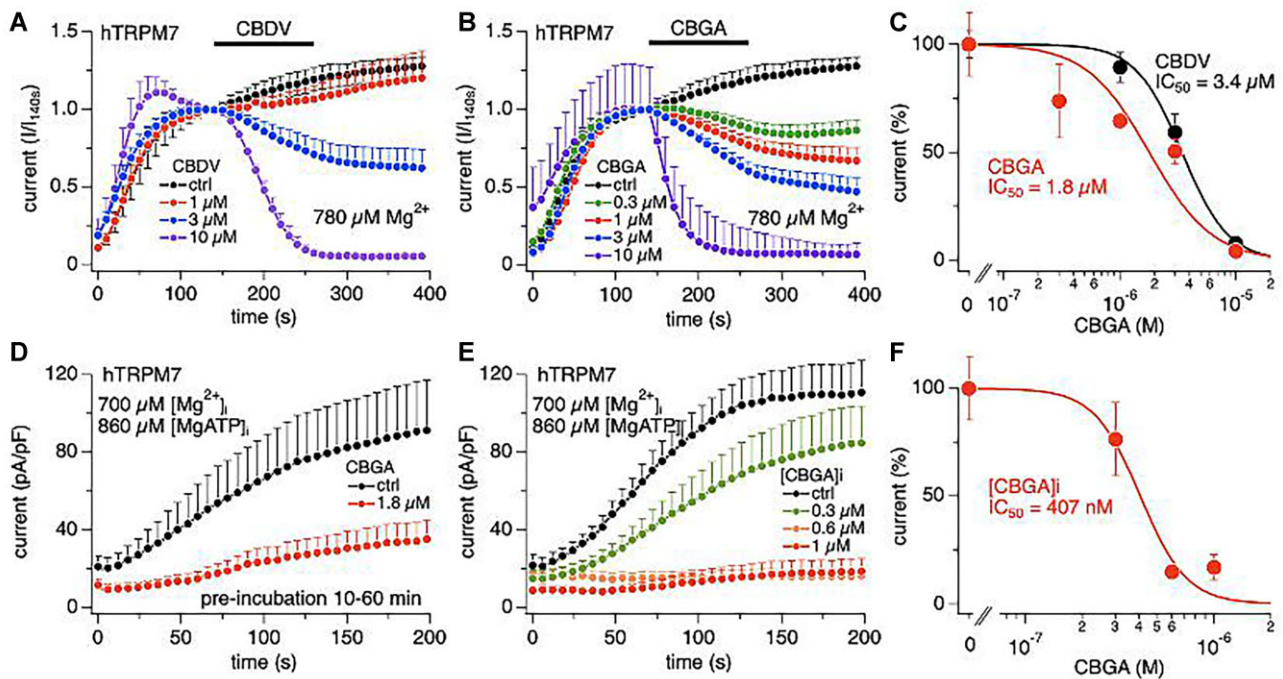
Figure 2. Cannabigerolic acid (CBGA) and cannabidivarin (CBDV) are a potent TRPM7 inhibitors. The inhibitory effect of CBDV and CBGA on TRPM7 current was assessed in whole-cell patch-clamp recordings on hTRPM7 overexpressed in HEK293 cells. The levels of free Mg^{2+} and Mg·ATP (if present) are indicated in the graphs. Cannabinoids were applied extracellularly at the indicated concentrations from 140 to 260 s (bars). Average TRPM7-mediated outward currents at +80 mV were extracted from ramp currents evoked by voltage ramps (−100 to +100 mV) delivered at 0.5 Hz and plotted as a function of time. The data points were normalized to the time point of cannabinoid application (140 s). (**A**) CBDV concentrations of 1 μM ($n = 7$), 3 μM ($n = 12$), and 10 μM ($n = 3$) were applied. Standard Ringer without cannabinoid contained acetonitrile as vehicle and was used as control ($n = 3$). (**B**) Cannabigerolic acid concentrations of 0.3 μM ($n = 24$), 1 μM ($n = 6$), 3 μM ($n = 6$), and 10 μM ($n = 3$) were applied. (**C**) Concentration-response curves of CBDV and CBGA on TRPM7 currents. Data points were obtained from the normalized currents in panels (**A**) and (**B**) at 260 s. Data fits yielded IC_{50} values for CBDV of 3.4 ± 0.2 μM and for CBGA of 1.8 ± 0.6 μM. (**D**) Cells were preincubated with either acetonitrile as vehicle control ($n = 16$) or 1.8 μM CBGA ($n = 13$) for 10-60 min prior to whole-cell recordings. (**E**) Cannabigerolic acid concentrations of 0.3 μM ($n = 7$), 0.6 μM ($n = 8$), and 1 μM ($n = 6$) were applied intracellularly. Standard intracellular solution without cannabinoid contained acetonitrile as vehicle and was used as control ($n = 5$). (**F**) Concentration-response curve of intracellular CBGA on TRPM7 currents. Data points were obtained from the normalized currents in panel (**E**) at 200 s. Data fit yielded an IC_{50} value for CBGA of 407 ± 46 nM.

preincubated cells with the previously calculated IC_{50} concentration of 1.8 μM CBGA for 10-60 min and then recorded TRPM7 currents in patch-clamp recordings. This resulted in a stronger than 50% inhibition (Figure 2D), suggesting that longer incubations allowed CBGA to approach steady state, but may still represent an underestimate as in whole-cell recordings with CBGA-free intracellular solutions CBGA could escape through the patch pipette and gradually alleviate the block. Therefore, we performed additional experiments in which we perfused CBGA directly into the cytosol by including it in patch pipette. Indeed, perfusing cells with increasing concentrations of CBGA potently suppressed TRPM7 currents, resulting in an IC_{50} value 407 nM (Figure 2F), suggesting that CBGA inhibits TRPM7 at submicromolar concentrations from the cytosolic side.

### Inhibitory Effect of CBGA is Selective for TRPM7 Over TRPM6

TRPM7 shares significant structural and functional characteristics with its sister channel TRPM6[22,43,44] and both can even form heteromeric assemblies with distinct properties.[45–47] TRPM6 and TRPM7 have distinct tissue distributions in that TRPM7 is ubiquitously expressed,[48] whereas TRPM6 is primarily expressed in the kidney and intestine, where it plays a significant role in magnesium reabsorption.[44] Both proteins are divalent-selective ion channels[39,47,49,50] and they both possess a functional kinase domain.[43,51] Their main functional differences are divergent

sensitivities to free Mg^{2+} and Mg·ATP. Thus, TRPM7 is negatively regulated by physiological levels of Mg·ATP,[39] whereas TRPM6 is largely insensitive to the adenine nucleotide complex[46] and heteromeric channels that include TRPM6 are much less sensitive to Mg·ATP.[45,46] Conversely, TRPM6 is exquisitely sensitive to even low micromolar free Mg^{2+} levels,[46] whereas TRPM7 is regulated by hundreds of micromolar levels.[37,39] To determine CBGA's selectivity for TRPM7, we assessed the effects of CBGA on TRPM6 channels transiently overexpressed in HEK293 cells.[46] TRPM6 currents activated extremely rapidly when perfused with Mg^{2+}-free intracellular solutions, likely due to the diffusional escape of cytosolic Mg^{2+} ions.[46] Applying 10 μM CBGA was completely ineffective in inhibiting fully activated TRPM6 currents (Figure 3A), whereas this concentration of CBGA completely blocks TRPM7 currents (see Figure 2B).

Unfortunately, TRPM6 channels cannot be recorded under the same experimental conditions as TRPM7 owing to their high sensitivity to free Mg^{2+}, so that these experiments were conducted with intracellular solutions devoid of free Mg^{2+} and Mg·ATP. As will be shown below, the absence of Mg^{2+} and Mg·ATP also greatly diminishes the efficacy of CBGA to inhibit TRPM7. For this reason, we investigated the effects of CBGA on heteromeric TRPM7/TRPM6 channels stably overexpressed in HEK293 cells and recorded with intracellular solutions containing 700 μM Mg^{2+} and 860 μM Mg·ATP. As illustrated in Figure 3B, increasing concentrations of CBGA inhibited these heteromeric channels, but with significantly lower potency than previously
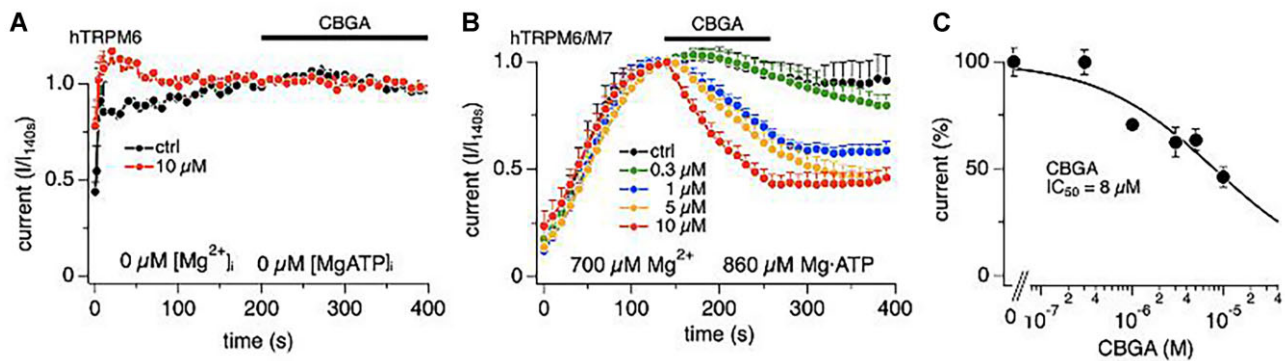
Figure 3. Homomeric TRPM6 and heterormeric channels of TRPM7 and TRPM6 are less sensitive to cannabigerolic acid (CBGA) inhibition. The same experimental protocol as in Figure 2B but recorded in HEK293 cells transiently overexpressing TRPM6 or stably transfected with heteromeric TRPM7 and TRPM6 channels. (**A**) TRPM6 currents in transiently transfected HEK293 cells evoked by perfusing cells with 0 Mg^{2+} and Mg·ATP. The data points were normalized to the time point before 10 μM CBGA ($n = 10$) application (200 s). Standard Ringer without cannabinoid contained acetonitrile as vehicle and was used as control ($n = 9$). (**B**) Heteromeric TRPM6/TRPM7 currents in stably transfected HEK293 cells. The data points were normalized to the time point before CBGA application (140 s). Concentrations of 0.3 μM ($n = 7$), 1 μM ($n = 7$), 5 μM ($n = 8$), and 10 μM ($n = 10$) were applied from 140 to 260 s (bar). Standard Ringer without cannabinoid contained acetonitrile as vehicle and was used as control ($n = 5$). (**C**) The concentration-response curve of CBGA on heteromeric TRPM7/TRPM6 currents ($IC_{50} = 8 \pm 2.5$ μM). Data points for the curve were obtained from the normalized currents in panel (**A**) at 260 s.
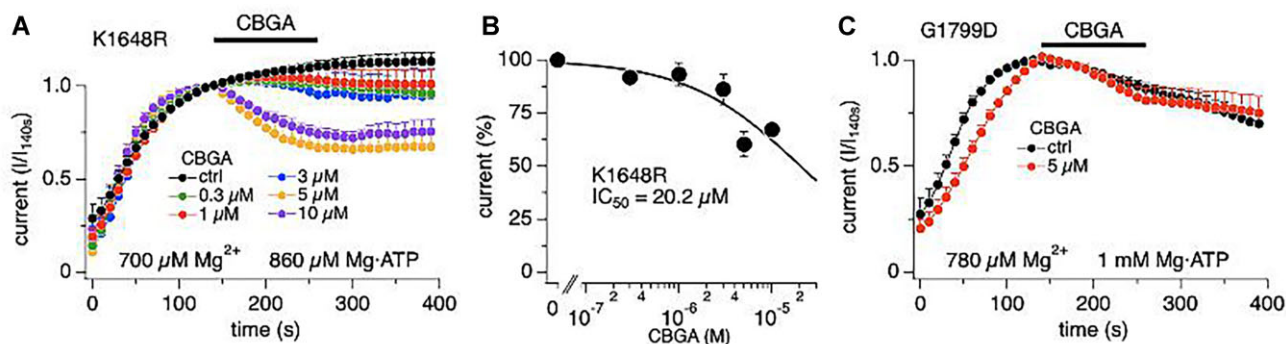
Figure 4. The inhibitory effect of cannabigerolic acid (CBGA) on TRPM7 requires a functional TRPM7 kinase domain. The same experimental protocol as in Figure 2B but recorded in HEK293 cells stable transfected with the phosphotransferase activity-deficient point mutations K1648R and G1799D. The levels of free Mg^{2+} and Mg·ATP are indicated in the graphs. (**A**) The data points were normalized to the time point before cannabinoid application (140 s). Concentrations of 0.3 μM ($n = 13$), 1 μM ($n = 12$), 3 μM ($n = 7$), 5 μM ($n = 7$), and 10 μM ($n = 7$) were applied from 140 to 260 s (bar). Standard Ringer without cannabinoid contained acetonitrile as vehicle and was used as control ($n = 7$). (**B**) The concentration-response curve of CBGA on K1648R TRPM7 currents ($IC_{50} = 20.2 \pm 12.9$ μM). Data points for the curve were obtained from the normalized currents in panel (**A**) at 260s. (**C**) The same experimental protocol as in Figure panel (**A**) but recorded in HEK293 cells stable transfected with the phosphotransferase activity-deficient point mutation G1799D. The data points were normalized to the time point before cannabinoid application (140 s). CBGA was applied at 5 μM ($n = 7$) and standard Ringer without cannabinoid contained acetonitrile as vehicle and was used as control ($n = 5$).

determined for TRPM7 (see Figures 2B and C), resulting in an IC_{50} value of 8 μM (Figure 3C) and suggesting that TRPM6 is much less or not at all susceptible to CBGA inhibition.

Inhibitory Effect of CBGA Requires a Functional Kinase Domain

The inhibitory effect of CBGA on TRPM7 is consistent with the previously described suppression observed in our acute nephropathic mouse model study.[28] Given the unique bifunctional properties of the protein (possessing both an ion channel function and protein kinase activity), we investigated whether CBGA inhibits TRPM7 via its endogenous kinase domain. Utilizing 2 HEK293 cell lines overexpressing phosphotransferase activity-deficient versions of human TRPM7 carrying point mutations K1648R or G1799D in the kinase domain.[40] Lysine residue K1648 is essential for Mg·ATP binding and its replacement with arginine K1648R results in a complete loss of a TRPM7 kinase activity.[40] Similarly, the glycine residue G1799

is thought to coordinate the Mg^{2+} ion of adenine nucleotides and its mutation to aspartic acid G1799D also results in loss of kinase activity. We examined the inhibitory effect of CBGA on both these mutants' currents. While 10 μM CBGA completely blocked TRPM7 currents in TRPM7/WT overexpressing HEK293 cells (92.4%, Figure 2B; purple), it inhibited the TRPM7/K1648R mutant cell line by just 36% (Figure 4A; purple). Moreover, CBGA concentrations of 0.3, 1, and 3 μM showed no significant inhibition of TRPM7 currents (Figure 4A; green, red, and blue circles, respectively), suggesting that an active kinase domain is required for CBGA inhibition. The IC_{50} of CBGA in the TRPM7/K1648R mutant was 20.2 ± 12.9 μM (Figure 4B), much higher than the TRPM7/WT value of 1.8 ± 0.6 μM and currents recorded from HEK293 cells overexpressing the other phosphotransferase-deficient mutant (G1799D) were completely unaffected by 5 μM CBGA (Figure 4C). Based upon these findings, we conclude that the potent CBGA-mediated inhibition of TRPM7 currents requires a functional TRPM7 kinase domain.

Inhibition of TRPM7 By CBGA is Sensitized By Mg^{2+} and Mg·ATP

Both Mg·ATP and Mg^{2+} are known to bind to the TRPM7 kinase domain and are critical for its phosphotransferase activity. Both also regulate TRPM7 channel function as they cause a reduction in TRPM7 channel activity.[37,39,40] As illustrated in Figure 4, CBGA was less effective at inhibiting TRPM7 currents in the TRPM7/K1648R point mutant cell line and completely ineffective in the TRPM7/G1799D mutant, prompting us to investigate whether the CBGA-mediated inhibition of TRPM7 was affected by intracellular levels of free Mg^{2+} and/or Mg·ATP. Figure 5A shows that at a physiological intracellular concentration of 780 μM free Mg^{2+}, 5 μM CBGA blocked 50% of TRPM7 currents with either 1 (Figure 5A; green) or 2 mM Mg·ATP (Figure 5A; blue) in HEK293 cells overexpressing hTRPM7/WT. However, omitting Mg·ATP dramatically limited the inhibitory effect of 5 μM CBGA on TRPM7 to just 6.8% (Figure 5A; black circles).

We next determined the inhibitory efficacy of 5 μM CBGA in the presence of various concentrations of free Mg^{2+} in the presence of a constant intracellular Mg·ATP concentration of 1 mM (Figure 5B). Free Mg^{2+} by itself will inhibit TRPM7 in a concentration-dependent manner (Figure 5D; black) with an IC_{50} of 883 ± 251 μM. The application of CBGA under these conditions did not significantly alter this relationship. In the presence of 5 μM CBGA, physiological levels of 780 μM free Mg^{2+} inhibited 50% of TRPM7 currents (Figure 5B; green), and 1 mM free Mg^{2+} slightly enhanced the inhibition of TRPM7 currents to 57% (Figure 5B; red). Conversely, lowering the concentration of free Mg^{2+} to 240 μM greatly diminished the inhibitory effect of CBGA to just 26% (Figure 5B; orange). The IC_{50} of intracellular free Mg^{2+} in the presence of 5 μM CBGA was calculated to be 878 ± 96 μM (Figure 5D; blue) in HEK293 cells overexpressing TRPM7/WT. This is very similar to the inhibition by free Mg^{2+} in the absence of CBGA, suggesting that a constant CBGA concentration does not significantly alter the Mg^{2+}-sensitivity of TRPM7.

To further probe the Mg^{2+}-dependence of CBGA, we examined whether CBGA requires Mg·ATP for Mg^{2+}-dependent TRPM7 inhibition. Here, we omitted 1 mM Mg·ATP from the intracellular medium and assessed the dose-response behavior at varying concentrations of intracellular free Mg^{2+}. Figure 5C illustrates that the inhibitory effect of 5 μM CBGA on TRPM7 was largely lost in the presence of both 780 μM (Figure 5C; green) and 240 μM free intracellular Mg^{2+} (Figure 5C; orange). However, CBGA's inhibitory effect on TRPM7 was partially restored at 1 mM free Mg^{2+}, at which concentration TRPM7 currents were again inhibited by 32% when exposed to 5 μM CBGA (Figure 5C; red). The above results demonstrate that the inhibitory effect of a constant dose of CBGA on TRPM7 is enhanced and sensitized by the presence of intracellular Mg^{2+} and Mg·ATP in a dose-dependent manner.

To further support the notion that the binding of Mg·ATP and/or Mg^{2+} to the kinase domain of TRPM7 is crucial to enable CBGA-mediated modulation of TRPM7 currents, we used HEK293 cells overexpressing the kinase-deficient TRPM7/K1648R point mutant. Here, 5 μM CBGA was less effective at suppressing TRPM7 currents in the kinase mutant cells when intracellular levels of free Mg^{2+} were progressively reduced from 1 mM (26%, Figure 5E; red), to 780 μM (19%, Figure 5E; green), and 240 μM (7%, Figure 5E; orange). Additionally, there was no inhibitory effect in Mg^{2+}-free conditions in the presence of 1 mM Mg·ATP in the TRPM7/K1648R overexpressing HEK293 cells (Figure 5E; black). Here, the TRPM7/K1648R mutant cells provided a higher IC_{50} value of intracellular free Mg^{2+} of 2.2 ± 0.7 mM (Figure

4D; red) as compared to 878 ± 96 μM in TRPM7/WT cells. Not surprisingly, under intracellular Mg·ATP-free conditions, the inhibitory effect of CBGA on TRPM7 currents was essentially absent, regardless of the free Mg^{2+} concentration in TRPM7/K1648R overexpressing HEK293 cells (Figure 5F). Taken together, these data suggest that the CBGA-mediated inhibition of TRPM7 currents not only requires a functional kinase domain, but also needs Mg·ATP and/or free Mg^{2+} to be effective.

$[Ca^{2+}]_i$ Reduces the Inhibitory Effect of CBGA on TRPM7

We have previously reported that TRPM7 regulates SOCE[52] and have recently demonstrated that CBGA suppresses IL-2 production in T cells through SOCE inhibition.[41] Therefore, we assessed the effect of intracellular calcium on CBGA's ability to inhibit TRPM7. The absence of intracellular free Ca^{2+} allowed 10 μM CBGA to completely block TRPM7 currents (Figure 6A; black) in hTRPM7/WT overexpressing cells. However, the presence of physiological free Ca^{2+} of 75 nM reduced the inhibitory effect of CBGA on TRPM7 to 48% (Figure 6A; blue), and this effect was exacerbated at higher free Ca^{2+} concentrations, where CBGA-mediated inhibition was reduced to 36% at 150 nM free Ca^{2+} (Figure 6A; red) and 33% at 300 nM free Ca^{2+} (Figure 6A; green). The EC_{50} of intracellular free Ca^{2+} concentration was 71 ± 3 nM (Figure 6B), right around resting levels of free Ca^{2+}.

Next, we investigated this effect of intracellular Ca^{2+} on HEK293 cells overexpressing the kinase-deficient K1648R mutant of TRPM7 in response to 10 μM CBGA. Figure 6C demonstrates that intracellular Ca^{2+}-free conditions were less efficient at reducing the inhibitory effect of 10 μM CBGA on TRPM7 in TRPM7/K1648R overexpressing cells (29%, Figure 6C; black) compared to TRPM7/WT overexpressing HEK293 cells (69%, Figure 6A; black). Unlike the situation in wild-type cells, increasing intracellular free Ca^{2+} to 150 nM in these TRPM7/K1648R overexpressing HEK293 cells maintained a 29% inhibition and failed to significantly affect the CBGA-mediated inhibition of TRPM7 (Figure 6C; red). Taken together, these results suggest that the efficacy of CBGA-mediated inhibition of TRPM7 decreases when intracellular free Ca^{2+} increases and, similarly to the free Mg^{2+} modulation, this effect appears to occur through the TRPM7 kinase domain.

CBGA Inhibits Native TRPM7 Currents in B Lymphocytes

The results presented above demonstrate that CBGA inhibits currents through TRPM7 channels heterologously overexpressed in HEK293 cells. We next investigated natively expressed, endogenous TRPM7 currents in the B lymphocyte myeloma cell line U266, where TRPM7 has previously been shown to be one of the main channels involved in multiple myeloma dissemination.[53] We assessed the inhibitory effect of CBGA on native TRPM7 activity in U266 cells in both in cell populations using fluorescence quenching of Fura-2 and in individual cells using the whole-cell patch-clamp technique. Since TRPM7 channels are constitutively active at low levels and conduct divalent cations such as Ca^{2+}, Mg^{2+}, Mn^{2+}, and Zn^{2+}, TRPM7 channel function can be assayed using Mn^{2+} as a surrogate for ion transport through TRPM7,[50,54] although cells have additional pathways that allow Mn^{2+} influx. Permeation of Mn^{2+} results in the fluorescence quenching of the calcium indicator Fura-2.[50,54,55] Using a kinetic plate reader, we monitored the real-time Mn^{2+} quenching of Fura-2 by various concentrations of CBGA in U266 cells. We used the TRPM7 inhibitor NS8593[30,52,56] as a positive control,
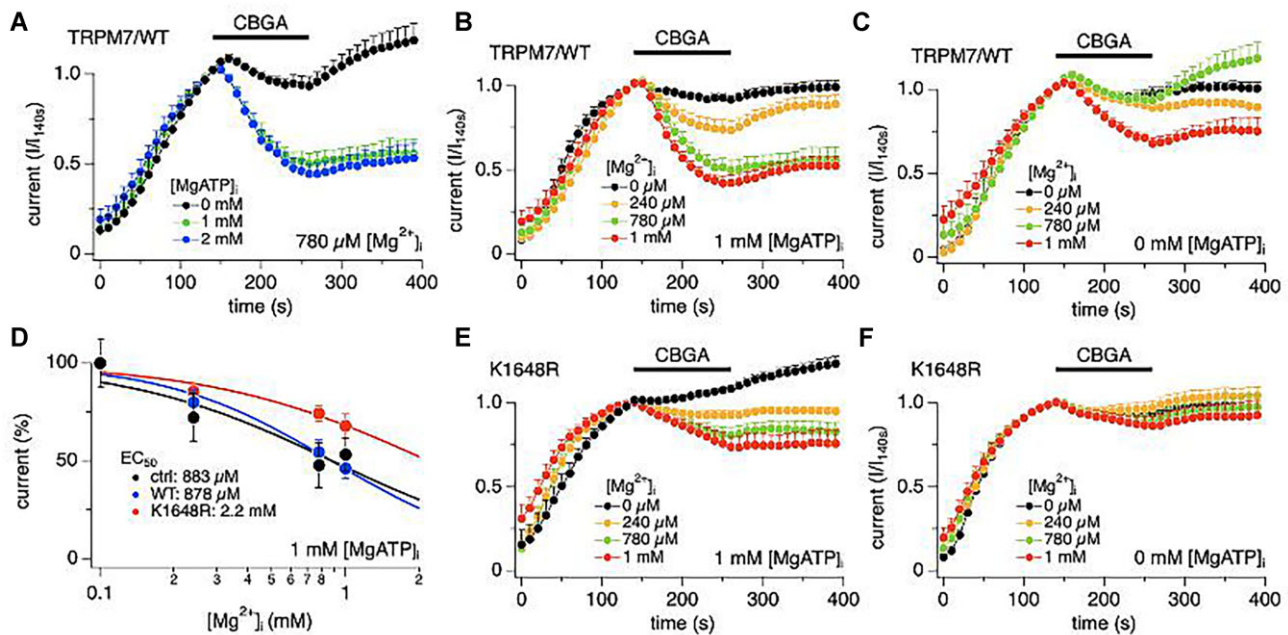
Figure 5. Cannabigerolic acid (CBGA) inhibits TRPM7 currents in an Mg·ATP- and Mg^{2+}-dependent manner. (**A**) The effect of Mg·ATP on suppression of TRPM7/WT currents by CBGA. The internal solution contained 780 μM intracellular free Mg^{2+} and additionally Mg·ATP concentrations of 0 mM ($n = 6$), 1 mM ($n = 6$), and 2 mM ($n = 6$). A 5 μM CBGA was applied from 140 to 260 s (bar). The data points were normalized to the time point before CBGA application (140 s). (**B**) The effect of free intracellular Mg^{2+} on the inhibition of TRPM7/WT currents by CBGA. The internal solution contained 1 mM Mg·ATP and additionally free Mg^{2+} concentrations of 0 μM ($n = 7$), 240 μM ($n = 6$), 780 μM ($n = 6$), and 1 mM ($n = 7$). A 5 μM CBGA was applied from 140 to 260 s (bar). (**C**) Same experimental protocol as in (**B**) but the internal solution contained 0 mM Mg·ATP and additionally free Mg^{2+} concentrations of 0 μM ($n = 4$), 240 μM ($n = 6$), 780 μM ($n = 6$), and 1 mM ($n = 7$). A 5 μM CBGA was applied from 140 to 260 s (bar). (**D**) Concentration-response curves of free Mg^{2+} on TRPM7/WT currents without CBGA ($EC_{50} = 883 \pm 251$ μM), on TRPM7/WT exposed to 5 μM CBGA in WT ($EC_{50} = 878 \pm 96$ μM), and on TRPM7/K1648R mutant (red; $EC_{50} = 2.2 \pm 0.7$ mM). Data points for the curves were obtained from the normalized currents in panels (**B**) and (**E**) at 260 s and at 140 s for WT control without CBGA. (**E**) The effect of free intracellular Mg^{2+} on the inhibition of K1648R currents by CBGA. The internal solution contained 1 mM Mg·ATP and additionally free Mg^{2+} concentrations of 0 μM ($n = 5$), 240 μM ($n = 7$), 780 μM ($n = 7$), and 1 mM ($n = 6$). A 5 μM CBGA was applied from 140 to 260 s (bar). (**F**) Same experimental protocol as in (**E**) but the internal solution contained 0 mM Mg·ATP and additionally free Mg^{2+} concentrations of 0 μM ($n = 5$), 240 μM ($n = 6$), 780 μM ($n = 6$), and 1 mM ($n = 7$). A 5 μM CBGA was applied from 140 to 260 s (bar).
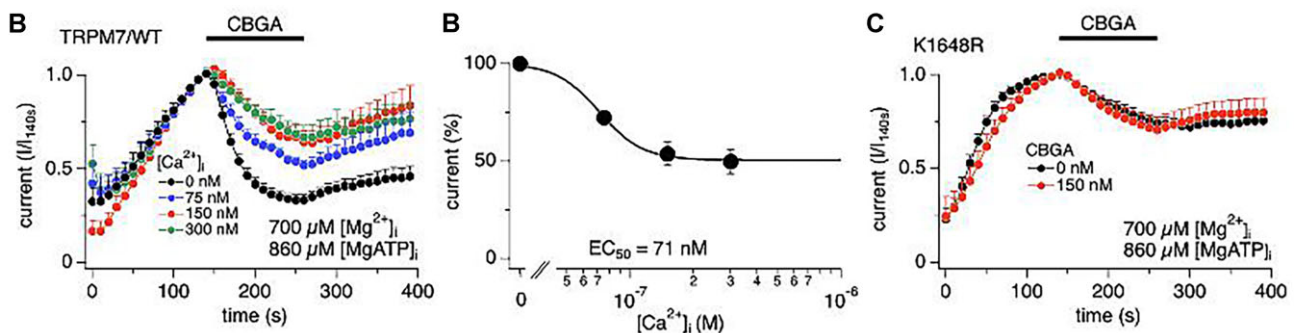
Figure 6. Calcium interferes with TRPM7 inhibition by cannabigerolic acid (CBGA). (**A**) The effect of intracellular free Ca^{2+} on TRPM7 inhibition by CBGA. The internal solution was buffered to free Ca^{2+} concentrations of 0 nM ($n = 6$), 75 nM ($n = 7$), 150 nM ($n = 7$), and 300 nM ($n = 7$) using 10 mM BAPTA and appropriate concentrations of $CaCl_2$. A 10 μM CBGA was applied from 140 to 260 s (bar). The data points were normalized to the time point before CBGA application (140 s). (**B**) The concentration-response curve of intracellular calcium to inhibit TRPM7 currents by 10 μM CBGA ($EC_{50} = 71 \pm 3$ nM). Data points for the curve were obtained from the normalized currents in panel (**A**) at 260 s. (**C**) The same experimental protocol as in (**A**) using 0 nM ($n = 7$) and 150 nM free Ca^{2+} ($n = 6$) in K1648R TRPM7 overexpressing HEK293 cells.

which at 10 μM suppressed 51% of the native TRPM7 activity in U266 cells. CBGA dose-dependently inhibited Mn^{2+} quenching of Fura-2 (Figure 7A) with an IC_{50} of 4.8 ± 1.1 μM (Figure 7B). Next, we assessed the inhibitory effect of CBGA on native TRPM7 currents in individual cells using the whole-cell patch-clamp technique. Here, 5 μM CBGA significantly blocked TRPM7 currents by 67% (Figures 7C and D; blue) and 10 μM CBGA completely blocked TRPM7 currents (Figures 7C and D; red) compared to vehicle control application (Figures 7C and D; black). These data suggest that

CBGA can suppress native TRPM7 channel activity at low micromolar concentrations.

Discussion

We have previously reported an interplay between TRPM7 and SOCE, where TRPM7 regulates SOCE through its kinase domain.[52] In addition, we have found that TRPM7 expression
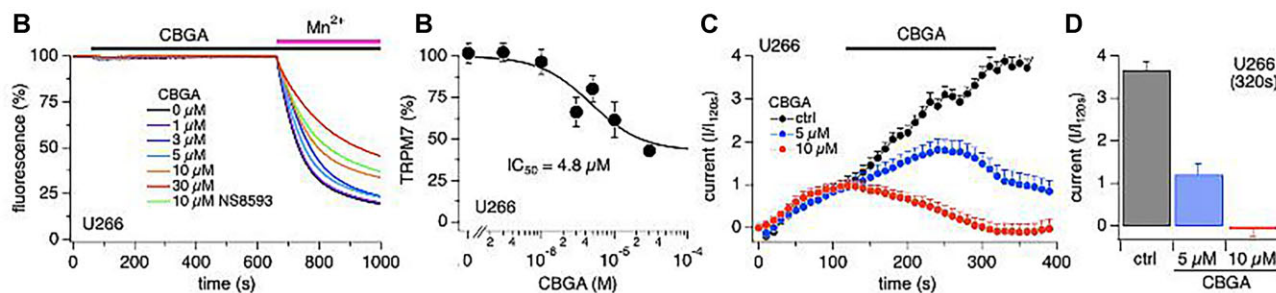
Figure 7. Cannabigerolic acid (CBGA) inhibits native TRPM7 currents in U266 cells. (**A**) U266 cells were used to investigate the inhibitory efficacy of CBGA in TRPM7-specific bioassay using fluorescence quenching of Fura-2 by Mn^{2+} influx (1 μM $GdCl_3$ was used to block Mn^{2+} entry through SOCE in all wells). Cells were were pretreated with various concentrations of CBGA for 10 mins (bar) and then exposed to 0.5 mM external $MnCl_2$ (bar) to induce fluorescence quenching. NS8593 was used as positive control to suppress TRPM7. (**B**) Concentration-response curve of CBGA on Mn^{2+}-mediated fluorescence quench in U266 cells. Data points for the curve were obtained from the normalized Fura-2 quench in (**A**) at 1000 s. Data fit yielded a half-maximal inhibitory concentration IC_{50} of 4.8 ± 1.1 μM. (**C**) Cannabigerolic acid inhibition of native TRPM7 currents in U266 cells using patch-clamp recordings. Cannabigerolic acid at concentrations of 5 μM ($n = 11$) and 10 μM ($n = 10$) were applied from 120 to 320 s (bar). Standard Ringer's solution without cannabinoid contained acetonitrile as vehicle and was used as control ($n = 6$). Data points were normalized to the time point before application of CBGA (120 s). (**D**) Bars reflect TRPM7 current amplitudes obtained from panel (**C**) at the end of CBGA application (320 s).

is upregulated in inflammatory renal damage and kidney fibrosis, and pharmacological intervention with the TRPM7 inhibitors NS8593[30] or CBGA[28] provide a reno-protective effect. In the present study, we identify and characterize the mechanism of action and the conditions that modulate the inhibitory effects of CBGA on TRPM7. This inhibitory effect requires a functional TRPM7 C-terminal kinase (Figures 4 and 5) and is concentration-dependently enhanced by intracellular Mg^{2+} and Mg·ATP acting at the kinase domain's Lys-1648 residue (Figure 5). We also determined that intracellular Ca^{2+} interferes with the efficacy of CBGA on TRPM7 activity (Figure 6), possibly by competing with Mg^{2+} at the kinase locus.

The presently most potent and selective TRPM7 inhibitor is waixenicin A, a marine-derived xenicane diterpene isolated from the soft coral *Sarcothelia edmondsoni*. Waixenicin A activity is regulated by intracellular free Mg^{2+}, and its potency reduced in TRPM7/K1648R overexpressing cells that harbor a point mutation in kinase domain.[54] This suggests that waixenicin A suppresses TRPM7 currents through Mg^{2+}-dependent mechanism at the kinase domain or a location that interacts with this domain. Our results show that CBGA appears to possess similar properties to waixenicin A in that CBGA synergizes with intracellular Mg^{2+} and Mg·ATP to block TRPM7 channel activity. We propose that intracellular free Mg^{2+} and Mg·ATP facilitate binding and coordination of the CBGA molecule at the kinase domain itself or some allosteric site that interacts with the kinase domain and ultimately results in inhibition of TRPM7 channel activity. While we have demonstrated a functional interplay of cannabinoids with Mg^{2+} and Mg·ATP and kinase domain mutations, we cannot rule out potential interactions and binding sites outside the kinase domain, including the possibility that the autophosphorylation status of the channel might be relevant.[51,57,58] Given the fact that a single point mutation in the cytosolic kinase domain essentially obliterates CBGA's ability to block TRPM7 indicates that a relatively nonspecific and more general membrane-delimited effect is unlikely. Thus, our data provide good circumstantial evidence for the requirement of a functional kinase activity rather than a direct demonstration that CBGA binds to the kinase domain at its catalytic sites, although this remains an intriguing scenario. This awaits additional biochemical/structural work akin to that provided for other agonists and antagonists of TRPM7.[59]

We previously reported CBGA inhibits SOCE by virtue of blocking CRAC channels subsequently suppressing IL-2 production in vitro and impeding the production of numerous inflammatory cytokines in vivo in mouse kidney.[41] Since TRPM7 can also modulate SOCE via its kinase activity, CBGA could have a dual effect on calcium influx by inhibiting SOCE directly and indirectly via TRPM7. Moreover, since the present study establishes that high intracellular Ca^{2+} interferes with the efficacy of CBGA's inhibitory action of TRPM7 activity (Figure 5), there may be yet another synergistic effect of CBGA in play. As CBGA can inhibit SOCE and reduce intracellular Ca^2 concentrations when stimulated, the reduction of intracellular Ca^{2+} would facilitate CBGA's suppression of TRPM7 channels and further suppress SOCE,[52] thereby providing a positive feedback loop to reduce SOCE-mediated inflammation. These interconnected inhibitory effects may be the underlying mechanisms that endow CBGA with strong anti-inflammatory properties.

Although both CBD and CBG appear to have anti-inflammatory effects in vivo[60]), we found that CBGA, but not CBD, suppressed mRNA expression of inflammatory cytokines and TRPM7 protein in a cisplatin-induced model of acute kidney injury.[28] Interestingly, CBD was generally ineffective in reducing most inflammatory markers and the combination of CBGA + CBD treatment reduced most mRNA levels similarly to CBGA treatment, although the suppressive effect was somewhat less in some cytokines, possibly indicating negative cooperativity effects of these cannabinoids when combined.[28] In patch-clamp experiments, we found that CBD didn't suppress TRPM7 currents[28] and in the present study, we found that the additional presence of 10 μM CBD did not significantly affect the IC_{50} of CBGA on TRPM7 currents. Interestingly, CBD nevertheless seemed to limit the total extent of CBGA-mediated inhibition to ~85%, which could help explain its apparent reduction of CBGA's inhibitory efficacy on TRPM7 in vivo in the nephropathic model.

Our manuscript provides data on the effects of CBGA, a compound that is generally regarded as safe and consumed by people as a nutraceutical. Its potency under physiological free Mg^{2+} and Mg·ATP conditions (intracellular IC_{50} of 407 nM) is higher than most other TRPM7 inhibitors (eg, NS8953[56] and VER155008[61]), with the possible exception of waixenicin A, which has an IC_{50} value in the low nanomolar range and exhibits a similar regulation by Mg^{2+} and nucleotides as CBGA[54] or

CCT128930,[62] which inhibits TRPM7 with IC_{50} values of 0.63 to 0.86 µM independently of intracellular free Mg^{2+} levels.[62] Interestingly, CCT128930 is a known ATP-competitive protein kinase B inhibitor, although its inhibitory activity on TRPM7 was proposed to involve residues near the TRPM7 selectivity filter rather than the kinase domain.[62] While some reports have claimed submicromolar IC_{50} values for NS8953 and VER155008 as well, they were either obtained through indirect measurements of Ca^{2+} entry induced by naltriben or under nonphysiological levels of 0 Mg^{2+} and MgATP in the presence of HEDTA (completely divalent-free). In intact cells under physiological conditions, where cytosolic levels of Mg^{2+} and Mg·ATP are in the hundreds of micromolar or several millimolar, NS8953 and VER155008 typically require several micromolar concentrations to exhibit significant effects.[30,56] Cannabigerolic acid exhibits submicromolar potencies when allowed longer exposure to gain cytosolic access or is administered intracellularly, where it inhibits with an IC_{50} of 407 nM (see Figures 2D-F).

While 10 µM CBGA is needed to achieve complete block, the IC_{50} is submicromolar when administered intracellularly and 1.8 µM when applied acutely, extracellularly, and for 120 s. Note that in our in vivo study on kidney disease,[28] we observed efficacy at 10 mg/kg i.p. injections. Pharmacokinetic data indicate that CBGA at that dose injected i.p. can reach Cmax values 64 µg/mL in plasma,[63] which is equivalent to 180 µM with a plateau of 20 µg/mL over 2 h. So even if one assumed poor bioavailability of 99% bound to serum albumins, one might still achieve low micromolar levels in plasma. Given the translocation into the cytosol and potential accumulation and retention, one might achieve effective levels of CBGA that can account for the observed biological effects,[28] although another study used CBGA at 30-100 mg/kg in their anticonvulsant assays.[17] While therapeutically effective dosing of CBGA is unknown, the maintenance dose of another cannabinoid (cannabidiol or CBG; Epidiolex) in humans is 25 mg/kg/d. Aside from its potential therapeutic value, CBGA appears to be a polyspecific inhibitor that targets CRAC channels and SOCE with submicromolar IC_{50} from the extracellular side[41] and TRPM7 with similar potency from the cytosolic side. Interestingly, both of these targets interact with each other in that TRPM7 plays a role in refilling intracellular stores and modulates CRAC channel activity via its kinase domain[52] and conversely, Ca^{2+} entry via CRAC channels would modulate the efficacy of CBGA in suppressing TRPM7 (see Figure 6).

In summary, CBGA can now be regarded as a potent submicromolar inhibitor of both SOCE via CRAC channels on the extracellular side as well as calcium and magnesium entry via TRPM7 channels on the cytosolic side. Inhibiting CRAC channels can have therapeutic potential in various medical conditions, primarily those involving immune system dysfunction or calcium dysregulation and particularly those in which lymphocytes play a prominent role. Some of the medical conditions in which CRAC channel inhibitors might be therapeutically useful include autoimmune and allergic disorders,[64,65] transplant rejection,[66] pancreatic diseases,[67] chronic pain,[68,69] and various cancers.[70-72] The additional inhibitory effects of CBGA on TRPM7 can not only potentiate the suppression of SOCE through the regulation of CRAC channels via its kinase domain,[52] but also offer additional therapeutic areas in which TRPM7 plays an important role of its own. This includes cardiac hypertrophy, arrhythmias, and vascular smooth muscle contraction,[27,73-75] neurological disorders such as Alzheimer's, Parkinson's, epilepsy stroke, and ischemia,[26,76-82] kidney disorders,[28,30,83,84] and various cancers.[23,36,85-89]

Conflict of Interest

The authors declare that they have no conflicts of interest with the contents of this article. A.F. holds the position of Editorial Board Member for *Function* and is blinded from reviewing or making decisions for the manuscript.

Data Availability

The data underlying this article will be shared on reasonable request to the corresponding author.

References

1. Urits I, Borchart M, Hasegawa M, et al. An update of current cannabis-based pharmaceuticals in pain medicine. *Pain Ther*. 2019;**8**(1):41–51.

2. Russo E. Cannabinoids in the management of difficult to treat pain. *Ther Clin Risk Manag*. 2008;**4**(1): 245–259.

3. Cassano T, Villani R, Pace L, et al. From cannabis sativa to cannabidiol: promising therapeutic candidate for the treatment of neurodegenerative diseases. *Front Pharmacol* 2020;**11**(124): 1–10.

4. Russo EB, Marcu J. Cannabis pharmacology: the usual suspects and a few promising leads. *Adv Pharmacol*. 2017;**80**:67–134.

5. Lewis M, Russo E, Smith K. Pharmacological foundations of cannabis chemovars. *Planta Med*. 2018;**84**(4):225–233.

6. Khan H, Ghori FK, Ghani U, et al. Cannabinoid and endocannabinoid system: a promising therapeutic intervention for multiple sclerosis. *Mol Biol Rep*. 2022;**49**(6):5117–5131.

7. Abd-Nikfarjam B, Dolati-Somarin A, Baradaran Rahimi V, et al. Cannabinoids in neuroinflammatory disorders: focusing on multiple sclerosis, parkinsons, and alzheimers diseases. *Biofactors*. 2023;**49**(3):560–583,

8. Haddad F, Dokmak G, Karaman R. The efficacy of cannabis on multiple sclerosis-related symptoms. *Life*. 2022;**12**(5):682.

9. Lazarini-Lopes W, Do Val-da Silva RA, da Silva-Júnior RMP, et al. Cannabinoids in audiogenic seizures: from neuronal networks to future perspectives for epilepsy treatment. *Front Behav Neurosci*. 2021;**15**(611902): 1–16.

10. Russo EB. Cannabis and epilepsy: an ancient treatment returns to the fore. *Epilepsy Behav*. 2017;**70**(Pt B)292–297.

11. Reddy DS. Therapeutic and clinical foundations of cannabidiol therapy for difficult-to-treat seizures in children and adults with refractory epilepsies. *Exp Neurol*. 2023;**359**:114237.

12. McDougall JJ, McKenna MK. Anti-inflammatory and analgesic properties of the cannabis terpene myrcene in rat adjuvant monoarthritis. *Int J Mol Sci*. 2022;**23**(14):7891.

13. Maayah ZH, Takahara S, Ferdaoussi M, et al. The anti-inflammatory and analgesic effects of formulated full-spectrum cannabis extract in the treatment of neuropathic pain associated with multiple sclerosis. *Inflamm Res*. 2020;**69**(6):549–558.

14. Zou S, Kumar U. Cannabinoid receptors and the endocannabinoid system: signaling and function in the central nervous system. *Int J Mol Sci*. 2018;**19**(3):833.

15. De Petrocellis L, Ligresti A, Moriello AS, et al. Effects of cannabinoids and cannabinoid-enriched *cannabis* extracts on TRP channels and endocannabinoid metabolic enzymes: novel pharmacology of minor plant cannabinoids. *Br J Pharmacol*. 2011;**163**(7):1479–1494.

16. Muller C, Morales P, Reggio PH. Cannabinoid ligands targeting TRP channels. *Front Mol Neurosci*. 2019;**11**:487.

17. Anderson LL, Heblinski M, Absalom NL, et al. Cannabigerolic acid, a major biosynthetic precursor molecule in cannabis, exhibits divergent effects on seizures in mouse models of epilepsy. *Br J Pharmacol*. 2021;**178**(24):4826–4841.

18. D'Aniello E, Fellous T, Iannotti FA, et al. Identification and characterization of phytocannabinoids as novel dual PPARα/γ agonists by a computational and in vitro experimental approach. *Biochim Biophys Acta Gen Subj*. 2019;**1863**(3):586–597.

19. Calapai F, Cardia L, Esposito E, et al. Pharmacological aspects and biological effects of cannabigerol and its synthetic derivatives. *Evid Based Complement Alternat Med*. 2022;**2022**(3336516): 1–14.

20. Burgaz S, García C, Gómez-Cañas M, et al. Neuroprotection with the cannabigerol quinone derivative VCE-003.2 and its analogs CBGA-Q and CBGA-Q-Salt in parkinson's disease using 6-hydroxydopamine-lesioned mice. *Mol Cell Neurosci* 2021;**110**(4): 103583.

21. Valdeolivas S, Navarrete C, Cantarero I, et al. Neuroprotective properties of cannabigerol in huntington's disease: studies in R6/2 mice and 3-Nitropropionate-lesioned mice. *Neurotherapeutics* 2015;**12**(1):185–199.

22. Fleig A, Chubanov V. TRPM7. *Handb Exp Pharmacol*. 2014;**222**:521–546.

23. Trapani V, Arduini D, Cittadini A, et al. From magnesium to magnesium transporters in cancer: TRPM7, a novel signature in tumour development. *Magnes Res* 2013;**26**(4): 149–155.

24. Nadolni W, Zierler S. The channel-kinase TRPM7 as novel regulator of immune system homeostasis. *Cells*. 2018;**7**(8):109.

25. Ryazanova LV, Rondon LJ, Zierler S, et al. TRPM7 is essential for Mg(2+) homeostasis in mammals. *Nat Commun*. 2010;**1**(1):109.

26. Chen W, Xu B, Xiao A, et al. TRPM7 inhibitor carvacrol protects brain from neonatal hypoxic-ischemic injury. *Molecular Brain*. 2015;**8**(1):11.

27. Du J, Xie J, Zhang Z, et al. TRPM7-mediated Ca2+ signals confer fibrogenesis in human atrial fibrillation. *Circ Res*. 2010;**106**(5):992–1003.

28. Suzuki S, Fleig A, Penner R. CBGA ameliorates inflammation and fibrosis in nephropathy. *Sci Rep*. 2023;**13**(1):6341.

29. Meng Z, Wang X, Yang Z, et al. Expression of transient receptor potential melastatin 7 up-regulated in the early stage of renal ischemia-reperfusion. *Transplant Proc*. 2012;**44**(5):1206–1210.

30. Suzuki S, Penner R, Fleig A. TRPM7 contributes to progressive nephropathy. *Sci Rep*. 2020;**10**(1):2333.

31. Guo J-L, Yu Y, Jia Y-Y, et al. Transient receptor potential melastatin 7 (TRPM7) contributes to H2O2-induced cardiac fibrosis via mediating Ca(2+) influx and extracellular signal-regulated kinase 1/2 (ERK1/2) activation in cardiac fibroblasts. *J Pharmacol Sci*. 2014;**125**(2):184–192.

32. Fang L, Huang C, Meng X, et al. TGF-β1-elevated TRPM7 channel regulates collagen expression in hepatic stellate cells via TGF-β1/Smad pathway. *Toxicol Appl Pharmacol*. 2014;**280**(2):335–344.

33. Yu M, Huang C, Huang Y, et al. Inhibition of TRPM7 channels prevents proliferation and differentiation of human lung fibroblasts. *Inflamm Res*. 2013;**62**(11):961–970.

34. Xu T, Wu B-M, Yao H-W, et al. Novel insights into TRPM7 function in fibrotic diseases: a potential therapeutic target. *J Cell Physiol*. 2015;**230**(6):1163–1169.

35. Middelbeek J, Kuipers AJ, Henneman L, et al. TRPM7 is required for breast tumor cell metastasis. *Cancer Res*. 2012;**72**(16):4250–4261.

36. Meng X, Cai C, Wu J, et al. TRPM7 mediates breast cancer cell migration and invasion through the MAPK pathway. *Cancer Lett*. 2013;**333**(1):96–102.

37. Demeuse P, Penner R, Fleig A. TRPM7 channel is regulated by magnesium nucleotides via its kinase domain. *J Gen Physiol*. 2006;**127**(4):421.

38. Kerschbaum HH, Kozak JA, Cahalan MD. Polyvalent cations as permeant probes of MIC and TRPM7 pores. *Biophys J*. 2003;**84**(4):2293–2305.

39. Nadler MJS, Hermosura MC, Inabe K, et al. LTRPC7 is a Mg·ATP-regulated divalent cation channel required for cell viability. *Nature*. 2001;**411**(6837):590–595.

40. Schmitz C, Perraud A-L, Johnson CO, et al. Regulation of vertebrate cellular Mg2+ homeostasis by TRPM7. *Cell*. 2003;**114**(2):191–200.

41. Faouzi M, Wakano C, Monteilh-Zoller MK, et al. Acidic cannabinoids suppress proinflammatory cytokine release by blocking store-operated calcium entry. *Function*. 2022;**3**(4):zqac033.

42. Storozhuk MV, Zholos AV. TRP channels as novel targets for endogenous ligands: focus on endocannabinoids and nociceptive signalling. *Curr Neuropharmacol*. 2018;**16**(2):137–150.

43. Schlingmann KP, Waldegger S, Konrad M, et al. TRPM6 and TRPM7—gatekeepers of human magnesium metabolism. *Biochim Biophys Acta Mol Basis Dis*. 2007;**1772**(8):813–821.

44. Chubanov V, Gudermann T. TRPM6. *Handb Exp Pharmacol*. 2014;**222**:503–520.

45. Ferioli S, Zierler S, Zaißerer J, et al. TRPM6 and TRPM7 differentially contribute to the relief of heteromeric TRPM6/7 channels from inhibition by cytosolic Mg2+ and Mg·ATP. *Sci Rep*. 2017;**7**(1):8806.

46. Zhang Z, Yu H, Huang J, et al. The TRPM6 kinase domain determines the Mg·ATP sensitivity of TRPM7/M6 heteromeric ion channels. *J Biol Chem*. 2014;**289**(8): 5217–5227.

47. Li M, Jiang J, Yue L. Functional characterization of homo- and heteromeric channel kinases TRPM6 and TRPM7. *J Gen Physiol*. 2006;**127**(5):525–537.

48. Fonfria E, Murdock PR, Cusdin FS, et al. Tissue distribution profiles of the human TRPM cation channel family. *J Recept Signal Transduct Res*. 2006;**26**(3):159–178.

49. Voets T, Nilius B, Hoefs S, et al. TRPM6 forms the Mg^{2+} influx channel involved in intestinal and renal Mg^{2+} absorption. *J Biol Chem*. 2004;**279**(1):19–25.

50. Monteilh-Zoller MK, Hermosura MC, Nadler MJS, et al. TRPM7 provides an ion channel mechanism for cellular entry of trace metal ions. *J Gen Physiol*. 2003;**121**(1):49–60.

51. Schmitz C, Perraud AL, CO J, et al. Regulation of vertebrate cellular Mg2+ homeostasis by TRPM7. *Cell*. 2003;**114**(2):191–200.

52. Faouzi M, Kilch T, Horgen FD, et al. The TRPM7 channel kinase regulates store-operated calcium entry. *J Physiol*. 2017;**595**(10):3165–3180.

53. Morelli MB, Amantini C. Transient receptor potential (TRP) channels: markers and therapeutic targets for cancer? *Biomolecules*. 2022;**12**(4):547.

54. Zierler S, Yao G, Zhang Z, et al. Waixenicin a inhibits cell proliferation through magnesium-dependent block of transient receptor potential melastatin 7 (TRPM7) channels. *J Biol Chem*. 2011;**286**(45):39328–39335.

55. Fasolato C, Hoth M, Penner R. Multiple mechanisms of manganese-induced quenching of fura-2 fluorescence in rat mast cells. *Pflugers Arch*. 1993;**423**(3–4):225–231.

56. Chubanov V, Mederos y Schnitzler M, Meißner M, et al. Natural and synthetic modulators of SK (K(ca)2) potassium channels inhibit magnesium-dependent activity of the kinase-coupled cation channel TRPM7. *Br J Pharmacol*. 2012;**166**(4):1357–1376.

57. Cai N, Lou L, Al-Saadi N, et al. The kinase activity of the channel-kinase protein TRPM7 regulates stability and localization of the TRPM7 channel in polarized epithelial cells. *J Biol Chem*. 2018;**293**(29):11491–11504.

58. Clark K, Middelbeek J, Morrice NA, et al. Massive autophosphorylation of the Ser/Thr-rich domain controls protein kinase activity of TRPM6 and TRPM7. *PLoS One*. 2008;**3**(3):e1876.

59. Nadezhdin KD, Correia L, Narangoda C, et al. Structural mechanisms of TRPM7 activation and inhibition. *Nat Commun*. 2023;**14**(1):2639.

60. Henshaw FR, Dewsbury LS, Lim CK, Steiner GZ. The Effects of Cannabinoids on Pro- and Anti-Inflammatory Cytokines: A Systematic Review of In Vivo Studies. *Cannabis Cannabinoid Res*. 2021;**6**(3):177–195.

61. Rössig A, Hill K, Nörenberg W, et al. Pharmacological agents selectively acting on the channel moieties of TRPM6 and TRPM7. *Cell Calcium*. 2022;**106**:102640.

62. Guan Z, Chen X, Fang S, et al. CCT128930 is a novel and potent antagonist of TRPM7 channel. *Biochem Biophys Res Commun*. 2021;**560**:132–138.

63. Anderson LL, Low IK, Banister SD, et al. Pharmacokinetics of phytocannabinoid acids and anticonvulsant effect of cannabidiolic acid in a mouse model of dravet syndrome. *J Nat Prod*. 2019;**82**(11):3047–3055.

64. Feske S, Skolnik EY, Prakriya M. Ion channels and transporters in lymphocyte function and immunity. *Nat Rev Immunol*. 2012;**12**(7):532–547.

65. Bakowski D, Murray F, Parekh AB. Store-operated Ca2+ channels: mechanism, function, pharmacology, and therapeutic targets. *Annu Rev Pharmacol Toxicol*. 2021;**61**(1):629–654.

66. McCarl C-A, Khalil S, Ma J, et al. Store-operated Ca2+ entry through ORAI1 is critical for t cell-mediated autoimmunity and allograft rejection. *J Immunol*. 2010;**185**(10):5845–5858.

67. Gerasimenko OV, Gerasimenko JV. CRAC channel inhibitors in pancreatic pathologies. *J Physiol*. 2022;**600**(7):1597–1598.

68. Tsujikawa S, DeMeulenaere KE, Centeno MV, et al. Regulation of neuropathic pain by microglial Orai1 channels. *Sci Adv*. 2023;**9**(4):eade7002.

69. Mei Y, Barrett JE, Hu H. Calcium release-activated calcium channels and pain. *Cell Calcium*. 2018;**74**:180–185.

70. Tiffner A, Hopl V, Derler I. CRAC and SK channels: their molecular mechanisms associated with cancer cell development. *Cancers*. 2022;**15**(1):101.

71. Shapovalov G, Gordienko D, Prevarskaya N. Store operated calcium channels in cancer progression. *Int Rev Cell Mol Biol*. 2021;**363**:123–168.

72. Jardin I, Rosado JA. STIM and calcium channel complexes in cancer. *Biochim Biophys Acta*. 2015;**6**(Pt B): 1418–1426

73. Rios FJ, Zou Z-G, Harvey AP, et al. Chanzyme TRPM7 protects against cardiovascular inflammation and fibrosis. *Cardiovasc Res*. 2020;**116**(3):721–735.

74. Antunes TT, Callera GE, He Y, et al. Transient receptor potential melastatin 7 cation channel kinase: new player in angiotensin II-induced hypertension. *Hypertension*. 2016;**67**(4):763–773.

75. Parajuli N, Valtuille L, Basu R, et al. Determinants of ventricular arrhythmias in human explanted hearts with dilated cardiomyopathy. *Eur J Clin Invest*. 2015;**45**(12): 1286–1296.

76. Sun Y, Sukumaran P, Schaar A, et al. TRPM7 and its role in neurodegenerative diseases. *Channels*. 2015;**9**(5): 253–261.

77. Zhang S, Cao F, Li W, et al. TRPM7 kinase activity induces amyloid-β degradation to reverse synaptic and cognitive deficits in mouse models of Alzheimer's disease. *Sci Signal*. 2023;**16**(793):eade6325.

78. Abumaria N, Li W, Clarkson AN. Role of the chanzyme TRPM7 in the nervous system in health and disease. *Cell Mol Life Sci*. 2019;**76**(17):3301–3310.

79. Sturgeon M, Wu P, Cornell R. SLC41A1 and TRPM7 in magnesium homeostasis and genetic risk for Parkinson's disease. *J Neurol Neuromedicine*. 2016;**1**(9): 23–28.

80. Khalil A, Shekh-Ahmad T, Kovac S, et al. Drugs acting at TRPM7 channels inhibit seizure-like activity. *Epilepsia Open*. 2023;**8**(3):1169–1174.

81. Turlova E, Wong R, Xu B, et al. TRPM7 mediates neuronal cell death upstream of calcium/calmodulin-dependent protein kinase II and calcineurin mechanism in neonatal hypoxic-ischemic brain injury. *Transl Stroke Res*. 2021;**12**(1): 164–184.

82. Aarts MM, Tymianski M. TRPM7 and ischemic CNS injury. *Neuroscientist*. 2005;**11**(2):116–123.

83. Lee C-T, Ng H-Y, Kuo W-H, et al. The role of TRPM7 in vascular calcification: comparison between phosphate and uremic toxin. *Life Sci*. 2020;**260**:118280.

84. Liu A, Yang B. Roles of TRPM7 in renal ischemia-reperfusion injury. *Curr Protein Pept Sci*. 2019;**20**(8):777–788.

85. Liu H, Dilger JP, Lin J. A pan-cancer-bioinformatic-based literature review of TRPM7 in cancers. *Pharmacol Ther*. 2022;**240**:108302.

86. Meng L, Gu G, Bi L. Transient receptor potential channels in multiple myeloma. *Oncol Lett*. 2022;**23**(4):108.

87. Ji D, Fleig A, Horgen FD, et al. Modulators of TRPM7 and its potential as a drug target for brain tumours. *Cell Calcium*. 2022;**101**:102521.

88. Meng S, Alanazi R, Ji D, et al. Role of TRPM7 kinase in cancer. *Cell Calcium*. 2021;**96**:102400.

89. Chinigò G, Fiorio Pla A, Gkika D. TRP channels and small GTPases interplay in the main hallmarks of metastatic cancer. *Front Pharmacol*. 2020;**11**:581455.